“Sudbury Breccia” at Whitefish Falls, Ontario: evidence for an impact origin

Andrew C. Parmenter, Christopher B. Lee, and Mario Coniglio

Abstract: Sudbury breccias are unusual clast–matrix rock bodies formed in abundance around the Sudbury Igneous Complex, the most obvious manifestation of a major impact event at Sudbury. At Whitefish Falls, ~70 km southwest of Sudbury, similar breccias consisting of clasts of argillite and amphibolite dyke enclosed in a fine-grained matrix of host rock are developed in metamorphosed argillites of the Huronian Supergroup. Pre-brecciation brittle textures in the host argillite and breccia clasts, such as layer-parallel foliation offset by cataclastic fractures, suggest that the host rock was entirely competent prior to brecciation. One composite penetrative foliation and its associated ductile folding were also formed in the argillite host prior to brecciation. Post-brecciation ductile deformation produced a regionally dominant east–west-trending foliation, and two late-stage folding events, and indicate a syn-Penokean age of brecciation. The breccias at Whitefish Falls are enriched in ferromagnesian minerals compared to adjacent, embayed and partially digested, host rock. Flow-foliated breccia matrices surround a highly rounded clast phase. These features are characteristic of impact-related pseudotachylyte, formed during extreme cataclasis and friction melting of the impacted host rock. We propose that these breccias formed by injection of a high-strain, pseudotachylytic melt, triggered by the Sudbury impact event, and focused along a blind superfault, coincident with a post-Penokean high-strain zone.

Résumé : Les brèches de Sudbury sont des amas peu ordinaires de roches à matrice clastique formés en abondance autour du complexe igné de Sudbury, ces amas sont la manifestation la plus évidente d’un événement d’impact majeur à Sudbury. À Whitefish Falls, ~70 km au sud du Sudbury, des brèches semblables, composées de clastes d’argilite et de dyke à amphibolite encaissés dans une matrice à grains fins de la roche-hôte, se sont développées en des argilites métamorphosées du Supergroupe de l’Huronien. Des textures cassantes prébréchification dans l’argilite hôte et les clastes de brèche, telles qu’une foliation parallèle aux couches décalée par des fractures cataclastiques, suggèrent que la roche hôte était tout à fait compétente avant la bréchification. Une foliation pénétrante composite et le plissement ductile qui lui est associé ont aussi été formés dans l’argilite hôte avant la bréchification. Une déformation ductile post-bréchification a produit une foliation régionale à tendance dominante est-ouest et deux événements de plissement tardifs, indiquant un âge syn-pénokéen pour la bréchification. Les brèches de Whitefish Falls sont enrichies de minéraux ferro-magnésiens par rapport à la roche hôte adjacente qui est découpée et partiellement digérée. Des matrices de brèches foliées par écoulement entourent une phase de clastes très bien arrondies. Ces traits sont caractéristiques d’une pseudotachylite d’impact, formée durant une très grande cataclase et une fusion par frottement de la roche hôte enclavée. Nous proposons que ces brèches aient été formées par l’injection de roche pseudotachylitique fondue, sous forte contrainte, déclenchée par l’événement d’impact de Sudbury et localisée le long d’une superfaille cachée coïncidant avec une zone de contraintes élevées d’âge post-pénokéen.

[Traduit par la Rédaction]

Introduction

“Sudbury breccias” are a group of unusual clast–matrix rock bodies in a wide range of rock types in the Huronian Supergroup of the Southern Province and the Superior Province of the Sudbury region. They are best developed around the Sudbury Igneous Complex (SIC) and decrease in abundance away from the SIC (e.g., Dressler 1984; Thompson and Spray 1994). The SIC represents the most obvious remnant of a major impact event at Sudbury (Dietz 1964; Grieve et al. 1991). Sudbury breccias typically consist of locally derived, rounded clasts, supported by a dark, fine-grained matrix, are irregularly shaped, and range in scale from centimetres to kilometres. Despite their variety in scale, type, and age of host rock and their wide-ranging distribution, similarities among various Sudbury breccias (e.g., clast shape and distribution, matrix textures, and contact relationships with their host rocks) suggest a common mode of genesis, namely

Received 2 October 2001. Accepted 12 February 2002. Published on the NRC Research Press Web site at http://cjes.nrc.ca on 17 July 2002.

Paper handled by S. Hanmer.

A.C. Parmenter,[1] C.B. Lee,[2] and M. Coniglio. Department of Earth Sciences, University of Waterloo, Waterloo, ON N2L 3G1, Canada.

[1]Corresponding author (e-mail: parmenter_a@hotmail.com).
[2]Present address: SRK Consulting, 580-800 Hornby Street, Vancouver, BC V6C 3B6, Canada.

 DOI: 10.1139/E02-006

Fig. 1. Simplified map of the geology of the Sudbury region. Numbers refer to some examples of Sudbury breccia throughout the Sudbury region. 1, east of Lake Wanapitae (Peredery and Morrison 1984); 2, Lake Temagami (Simony 1964); 3–5, Superior Province northeast of the Sudbury Igneous Complex (Thompson and Spray 1994); 6 and 7, East Bull Lake and Shakespeare–Dunlop intrusions (Chubb et al. 1994); 8, Emo, Rhodes, and Botha townships (Dressler 1979); 9, Whitefish Falls (Card 1984; this study) (modified from Bennett et al. 1991; Spray and Thompson 1995).

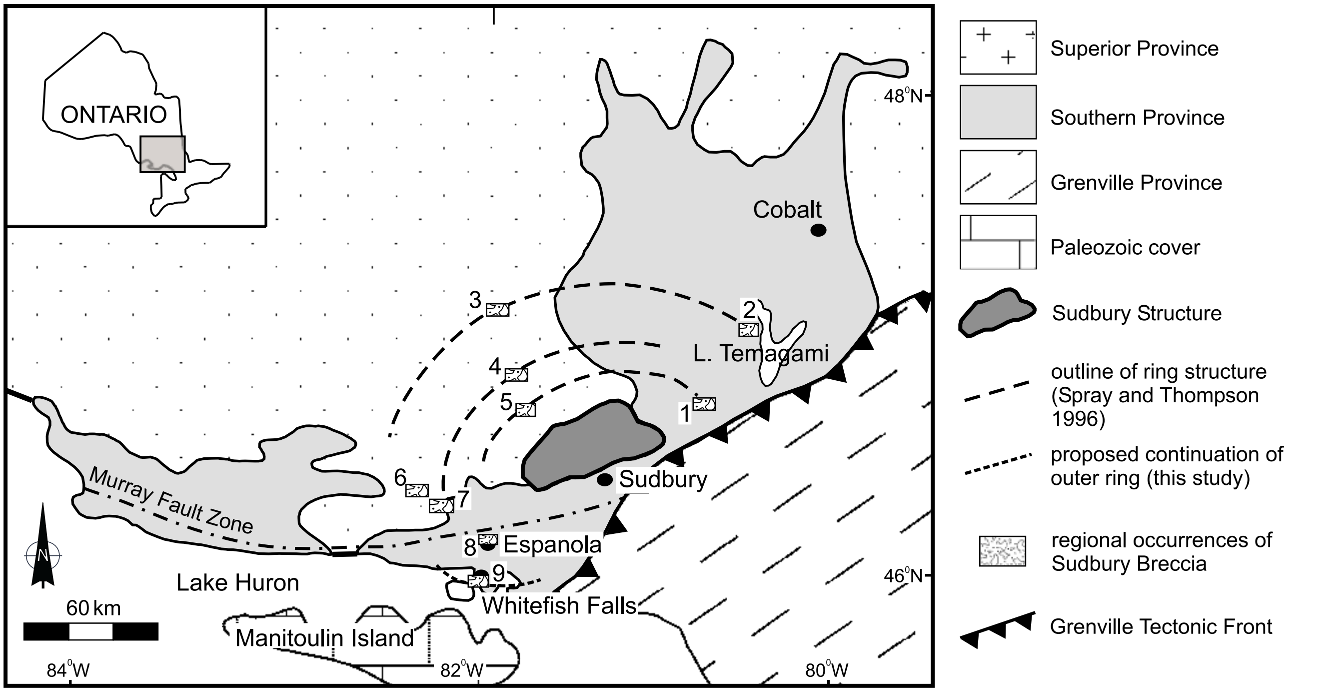

the Sudbury impact event (Dressler 1984; Grieve et al. 1991; Thompson and Spray 1994). This interpretation is not shared by all, however, based on local relationships that suggest alternative explanations (e.g., Shaw et al. 1999).

A discrepancy among the various brecciation models (Thompson and Spray 1994; Shaw et al. 1999; Lowman 1999) is the timing of breccia emplacement with respect to lithification, regional orogenesis, and the development of tectonic fabrics (Fig. 2). This study adds to the discussion, through a reexamination of the well-known Sudbury breccia occurrences in the area of Whitefish Falls, Ontario, ~80 km southwest of the SIC (Fig. 1).

Geological setting

Sudbury breccias in the Whitefish Falls area are hosted by metasedimentary rocks of the Huronian Supergroup, the distribution of which defines the Southern Province, bounded by the Superior Province and the Grenville Province to the north and southeast, respectively (Fig. 1) (Bennett et al. 1991; Rousell et al. 1997). Major depositional, intrusive, and tectonic events occurring in the Southern Province are summarized in Fig. 2.

The Huronian Supergroup is composed of three cyclical successions of glaciogenic continental margin sediments overlying basal mafic volcanics and related sedimentary rocks (Card 1978). All sedimentary and intrusive rocks within the Huronian Supergroup, except the Late Proterozoic Sudbury diabase dykes (below), have been metamorphosed, therefore, the prefix "meta" is implied throughout (e.g., Bennett et al. 1991). The basal volcanic succession is thought to be comagmatic with the ca. 2480 Ma (Krogh et al. 1984) East Bull Lake intrusions (Bennett et al. 1991). The ca. 2477 Ma (Krogh et al. 1996) Murray Pluton and the ca. 2333 Ma (Frarey et al. 1982) Creighton Pluton intrude the basal volcanics. The entire Huronian sequence is intruded by the ca. 2219 Ma (Corfu and Andrews 1986) Nipissing diabase (Card 1978).

Nipissing diabase intrusions are typically east-northeast trending, reach a maximum width of 460 m, and are intruded by north- to northwest-trending hornblende-bearing dykes (hereafter referred to as amphibolite dykes), ranging in width from 2 to 30 m (Card 1978, 1984). The absolute age of the amphibolite dykes is unknown, but they are transected by a regionally developed foliation (this study). Shaw et al. (1999) suggest that some of the amphibolite dykes in the Whitefish Falls area predate the Nipissing diabase. Both dykes are cut by the Middle Proterozoic, northwest-trending, ca. 1238 Ma (Krogh et al. 1987) Sudbury diabase, which ranges in thickness from a few metres to several hundred metres and transects major folds and the regional foliation (Card 1984).

The Sudbury–Manitoulin area consists of regional-scale, east- to northeast-trending, open to tight anticlines and synclines (Card 1978), which formed during the Blezardian orogeny (Stockwell 1982) and the Penokean orogeny (Card 1978; Bennett et al. 1991). Blezardian deformation is thought to have been initiated at ~2400 Ma (Riller et al. 1999) and may have affected both consolidated and unconsolidated sediments (Card 1978, 1984; Riller et al. 1999). Nipissing diabase intrusions cut all early structures, indicating termination of the Blezardian orogeny by ca. 2219 Ma (Riller et al. 1999). Penokean deformation overprinted Blezardian structures,

Fig. 2. Chronological summary of the geological history of the Sudbury region, correlated with the local geological history at Whitefish Falls. Proposed ages of Sudbury breccia formation, in relation to possible brecciation mechanism, are indicated. Vertical line fill indicates major orogenic events, and solid grey fill intrusive events. Citations are referred to in the text.

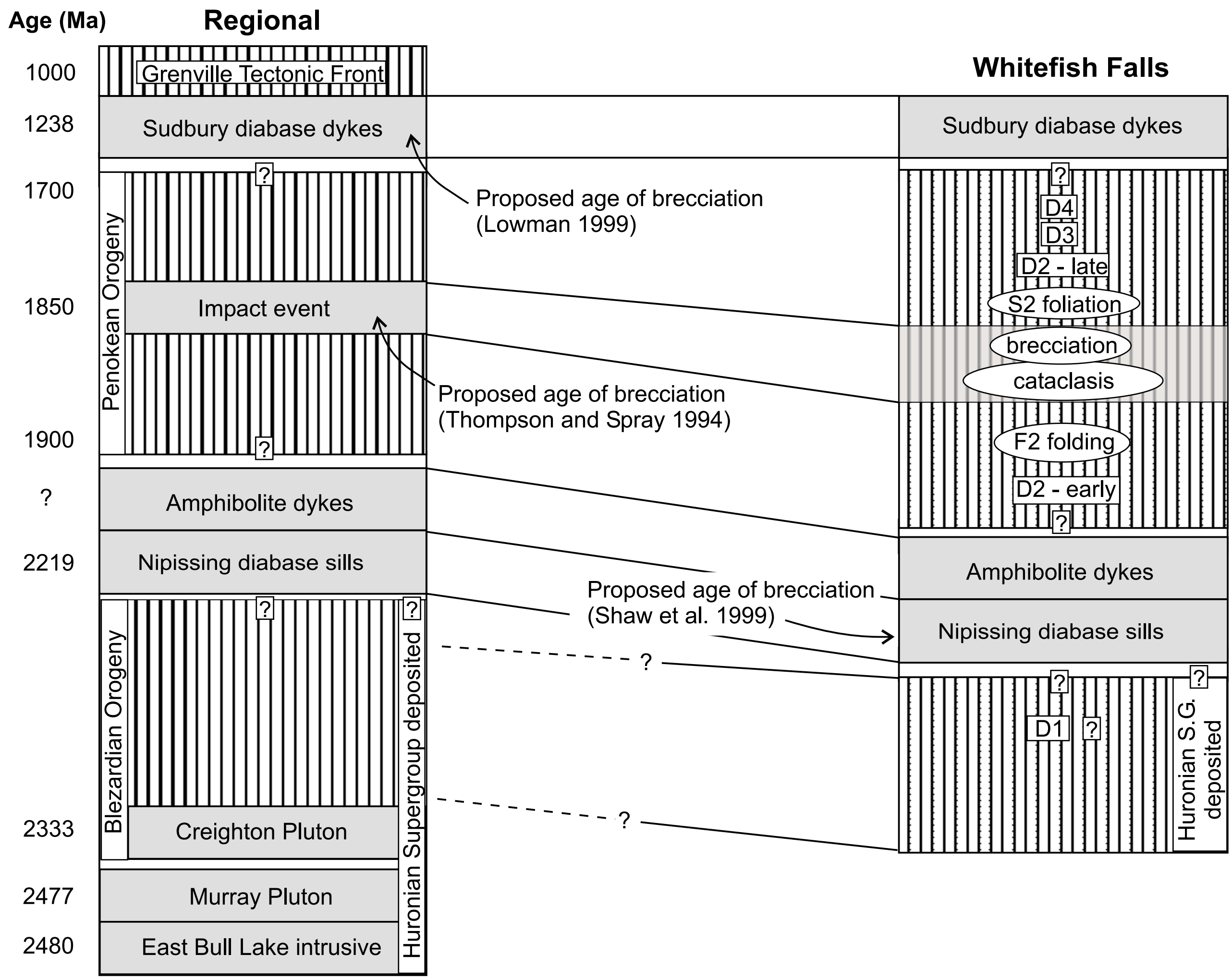

producing tight, doubly plunging, upright folds (Card 1984; Zolnai et al. 1984; Riller et al. 1999). The development of an east-trending cleavage, axial planar to these folds, is characteristic of late-stage Penokean deformation (Zolnai et al. 1984) and is clearly recognized in the Whitefish Falls area (Card 1978, 1984; this study). The Murray Fault Zone, an east-northeast-trending structure in the Sudbury region (Fig. 1), was the locus of dextral transpressive shortening throughout the Penokean orogeny (Zolnai et al. 1984; Riller et al. 1999). Various age estimates of Penokean orogenesis suggest a maximum deformation interval between ca. 1900 and 1700 Ma (Bennett et al. 1991). The 1850 Ma (Krogh et al. 1984) Sudbury impact event occurred during this interval.

Advance of the Grenville Province towards the Southern Province (ca. 1000 Ma; Bennett et al. 1991) displaced Sudbury diabase dykes in close proximity to the tectonic front (Condie et al. 1987; Rousell et al. 1997) but did not affect similar dykes at Whitefish Falls, ~50 km to the east.

Field and petrographic observations

The local stratigraphy represents the central portion of the Huronian Supergroup (Fig. 3). The metasedimentary rocks are intruded by northwest-trending amphibolite dykes. The dyke – host rock contacts are generally sharp and well defined, except through the centre of the map area where continuity of both the laminated argillite and the dykes is disrupted and Sudbury breccia is developed (Fig. 3). Continuous, north-northwest-trending Sudbury diabase dykes cut across the entire map area (Fig. 3).

Deformation history

Four episodes of deformation (D1, D2, D3, and D4) define three tectonic foliations (S1, S2, and S3) and three folding events (F2, F3, and F4).

D1 produced a penetrative, bedding-parallel S0/S1 composite foliation (S0/S1), defined by quartz, sericite, biotite, and chlorite (Fig. 4*a*). S0/S1 is recognized in the argillite and laminated argillite (Fig. 3) but was not identified in other sedimentary units or the dykes. S0/S1 is transposed by later deformation and is only preserved in the hinges of younger folds.

D2 produced an east-trending, spaced crenulation cleavage (S2) (Figs. 4*a*, 4*b*). S2 is defined by a preferred orientation

Fig. 3. Simplified geology of Whitefish Falls, highlighting the distribution of Sudbury breccia through the middle of the laminated argillite of the Gowganda Formation (modified from Young 1983). The box west of Highway 6 indicates the approximate area shown in Fig. 5.

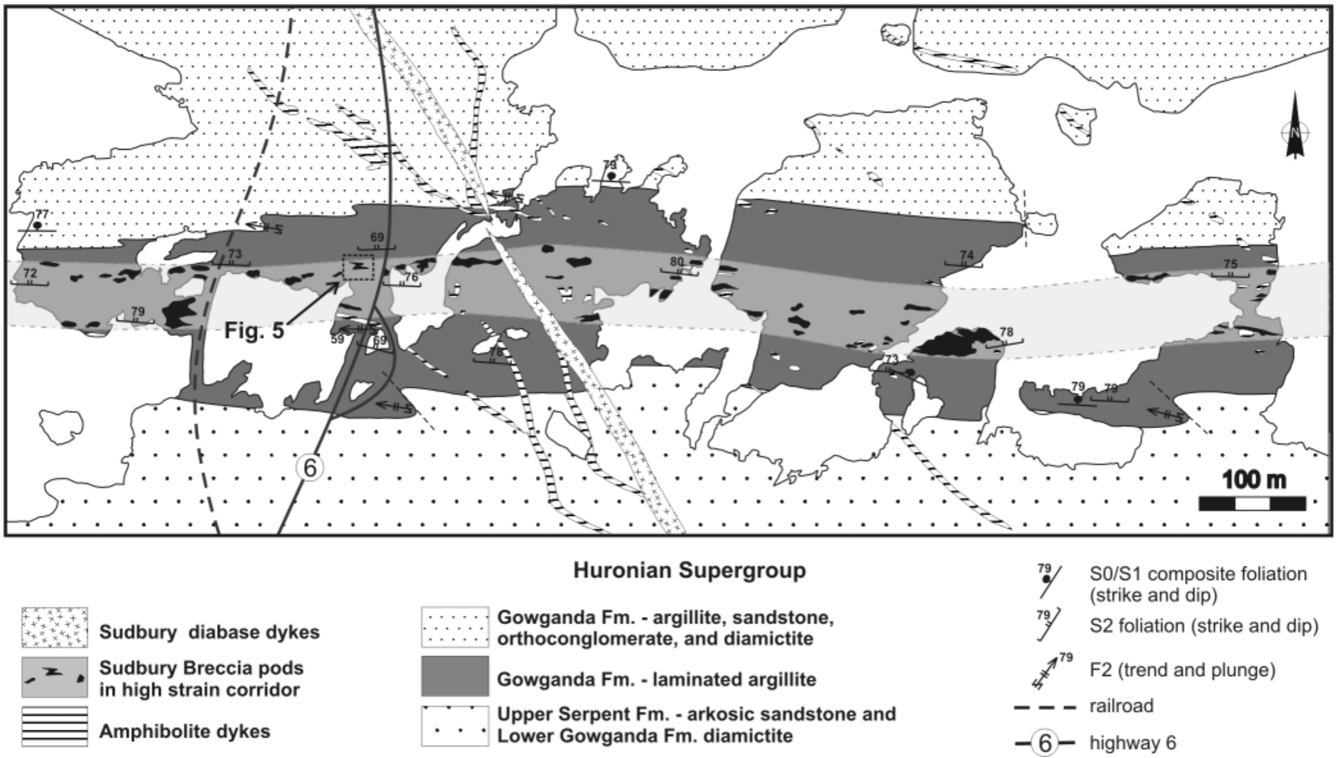

of fine- to coarse-grained biotite crystals in discrete cleavage domains, within the argillite and laminated argillite. The average S2 orientation is 276/83. S2 is not evident in the diamictite, quartzite, or arkose units (Fig. 3), but their bedding contacts are approximately parallel to the S2 foliation trend. S2 overprints the amphibolite dykes (Fig. 4*c*).

The S2 foliation is axial planar to concentric F2 folds in the argillite and tight, similar folds in the laminated argillite (Fig. 4*b*). Transposition of pre-D2 structures in the F2 fold limbs produced a composite S0/S1/S2 foliation. S folds without axial-planar cleavage are observed at all main lithological contacts (Fig. 3). These folds are also attributed to D2.

D3 produced rare F3 folds, with a locally developed axial-planar fabric (S3). F3 folds are defined by centimetre-scale, chevron-type folding of the S2 foliation (Figs. 4*d*, 4*e*). They are only observed in the argillite and laminated argillite, where they affect the S2 foliation. S3 was observed only in one locality, in the hinge of a minor F3 fold. It is a spaced crenulation cleavage, which sharply offsets bedding planes and the S1/S2 penetrative foliations. The amphibolite and Sudbury diabase dykes show no discernible F3 effects.

D4 produced rare F4 folds, with no associated axial-planar foliation. F4 folds are defined by reorientation of the S2 foliation into clusters of parallel, 1–20 cm wide, S-shaped kink bands, concentrated into zones up to 3.5 m wide. The kink bands form in the hinge area of larger concentric S folds (Figs. 4*d*, 4*e*). Like F3 folds, F4 folds are only observed in the argillite and laminated argillite units. The amphibolite and Sudbury diabase dykes show no clear F4 effects.

Sudbury breccias

Sudbury breccias are developed in a 150–200 m wide, S2-parallel, high-strain zone in the central portion of the laminated argillite (Fig. 3), characterized by disrupted bedding, amphibolite dyke discontinuity, irregular quartz veins, abundant cataclasis, and an intensified S2 foliation. The breccia occurs in pods, up to 70 m wide (most range between 2 and 10 m) and with sharp margins that cut the adjacent unbrecciated host rocks (Fig. 5). The breccia–argillite contacts are commonly rounded, especially where thin arms of breccia branch away from larger pods (Figs. 5, 7*a*). The pods are composed of two distinct phases: 5–80% predominantly locally derived clasts, and a fine-grained to aphanitic matrix. All breccia occurrences are preferentially elongate parallel to, and are overprinted by, the S2 foliation.

Matrix

The matrix is dominated by a fine-grained groundmass (average grain size ~5 μm) of quartz–feldspar–opaque–sericite–biotite–chlorite, surrounding larger crystals and fine-grained aggregates of quartz and feldspar. The matrix occurs locally as thin injection apophyses or embayments into the host rocks and the clasts (Figs. 6*a*, 6*b*). In thin section, these matrix embayments show a marked reduction of both ferromagnesian minerals (e.g., biotite and chlorite) and grain size relative to the surrounding matrix and unbrecciated host rock (Fig. 6*b*).

The matrix is generally massive but may exhibit a continuous, compositional flow foliation, defined by thin (<1 mm) layers

Fig. 4. Fabric and structural overprinting relationships in the laminated argillite and within clasts in the breccia matrix. (*a*) Thin-section photomicrograph of the S0/S1 composite foliation (solid line) transposed into the S2 foliation (broken line) orientation. (*b*) F2 fold in the argillite, overprinted by the axial-planar S2 foliation (broken line). Marker pen for scale. (*c*) Thin amphibolite dyke *d* cut by the S2 foliation (broken line). Note the refraction of S2 through the dyke. Pencil for scale. (*d*) F2, F3, and F4 fold overprinting relationship in the argillite. Scale card divisions in centimetres. (*e*) Sketch of area in (*d*), showing S2 foliation and F2 fold axial plane (broken line), F3 fold axial plane (line with widely spaced dots), and F4 fold axial plane (line with closely spaced dots).

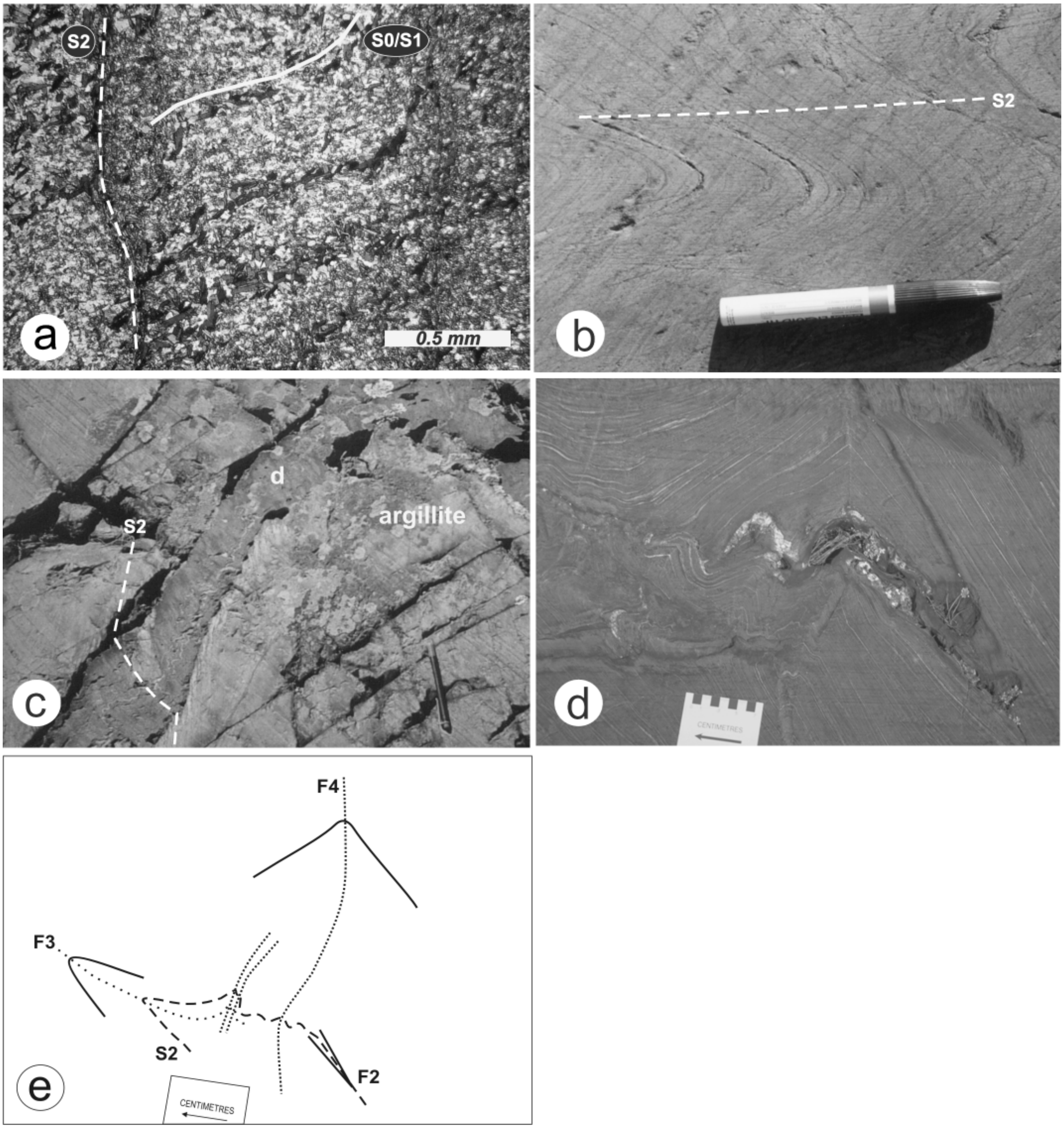

of altered biotite, alternating with 1–2 mm wide felsic layers. This foliation may be continuous for up to 1 m, outlining chaotic folds between the breccia clasts (Fig. 6*c*). Four distinct foliation layers (Fig. 6*d*) are distinguished: (*i*) quartz rich and sericite poor, with minor opaque minerals; (*ii*) sericite rich, with chlorite ± biotite; (*iii*) biotite rich, with minor

Fig. 5. Sketch map of breccia outcrop (location shown in Fig. 3) in the laminated argillite that highlights several important textural features and timing relationships. The S2 foliation overprints the entire outcrop (note average S2 orientation). Also indicated are the locations of Figs. 7*a*, 8*b*, 8*c*, and 8*d*.

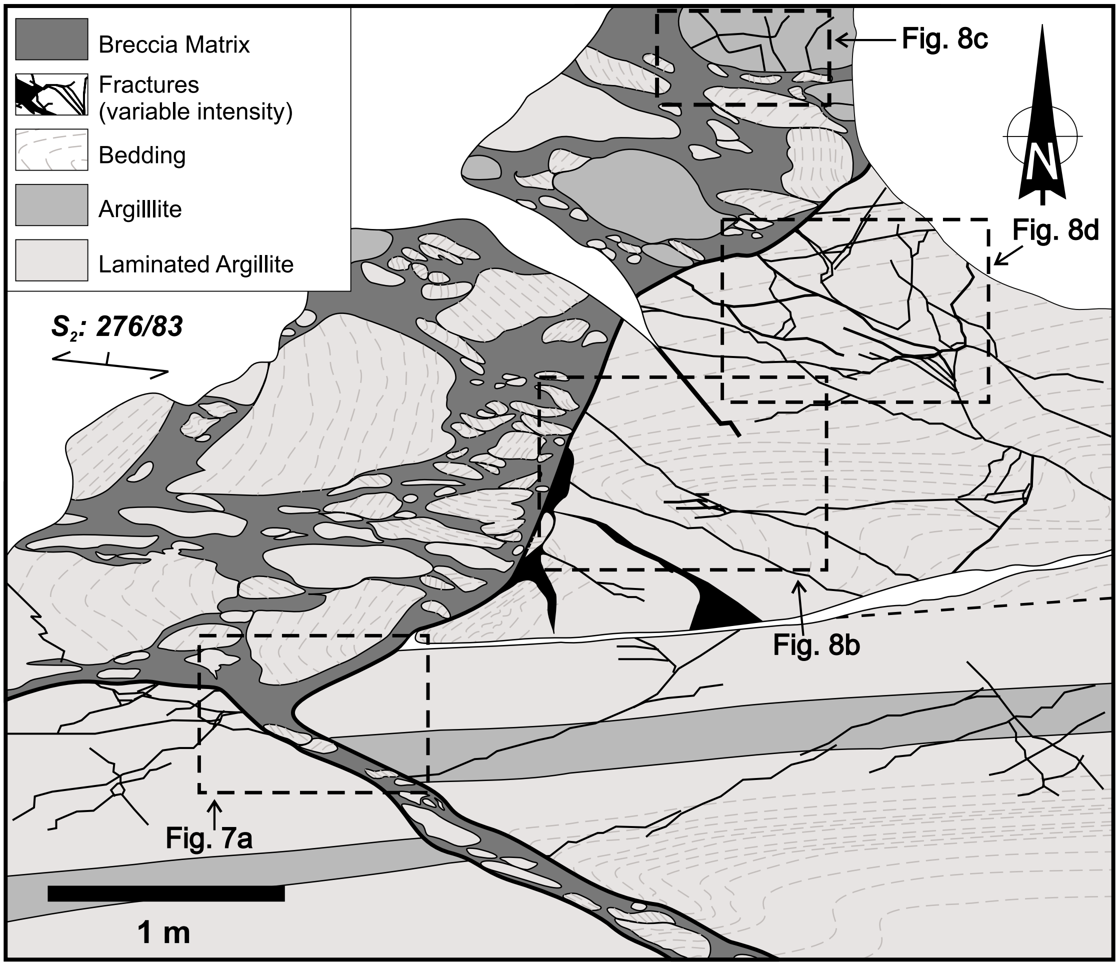

quartz; and (*iv*) chlorite rich. Grain sizes in these layers typically range from 3 to 15 μm. Quartz and feldspar mineral clasts, fine-grained quartz–feldspar aggregates, and biotite–chlorite aggregates embedded between foliation layers may reach up to 2 mm in size.

Lithic clasts

Clasts (<1 cm to >3 m in size) are usually derived from the adjacent host rock, irrespective of lithology. In some localities, however, “exotic” clasts whose source rock may be up to 100 m away in outcrop are present in minor amounts. Exotic clasts are most commonly amphibolite (estimated <3% of all clasts), and to a lesser extent very mature quartzite from the Lorraine Formation.

Clasts are preferentially elongate subparallel to, and overprinted by, the S2 foliation (Fig. 7*a*) and are occasionally concentrated into clast-supported, funnel-shaped zones exhibiting a tight mosaic, with very little interstitial matrix. Argillite clasts have an average aspect ratio of 2:1 with well-rounded margins (Figs. 6*c*, 7*b*). Amphibolite clasts have an average aspect ratio of 1:1 and are commonly rounded (Figs. 7*e*, 7*f*) but can also be irregular (Fig. 7*d*).

The argillite clasts typically display a well-preserved, bedding-parallel foliation (S0/S1) (Fig. 7*b*). S0/S1 is randomly oriented within adjacent clasts and with respect to the S2 foliation and is sharply truncated at clast–matrix contacts (Figs. 6*c*, 7*b*). The S2 foliation locally transects a folded S0/S1 foliation within the clasts (Fig. 7*c*).

Amphibolite clasts exhibit sharp to diffuse contacts with the surrounding matrix (Figs. 6*a*, 7*e*). They show no evidence of an intrusive origin (e.g., fine-grained chilled margin and coarse-grained centre), and grain size is commonly coarse from centre to margin (Fig. 7*e*). Concentrations of amphibolite dyke clasts coincide with nearby occurrences of in situ amphibolite dykes.

Both argillite and amphibolite clasts typically exhibit lightened or “blanched” margins (0.25–1.5 cm wide) at their contacts with the matrix (Figs. 6*a*, 6*c*, 7*b*). Blanching also occurs along wispy layers that have been entrained into the surrounding matrix. Blanching is most apparent in areas where flow foliation is developed, and along matrix apophyses in amphibolite clasts (Fig. 6*a*).

The blanched margin is characterized by a decrease in grain size (average 2–5 μm) relative to both the breccia matrix and the clasts, and commonly by a decrease in the percentage of ferromagnesian minerals relative to the matrix. Blanching along argillite clast margins produces a distinct segregation between the ferromagnesian and quartz–feldspar-rich layers,

Fig. 6. Matrix textures and clast–matrix relationships. (*a*) Breccia matrix injection into an amphibolite dyke clast. Note the blanching at the clast–matrix contact. Mechanical pencil for scale. (*b*) Thin-section photomicrograph of a matrix embayment in an amphibolite dyke clast. Note the marked colour and grain-size contrast between the biotite-poor – quartz-rich embayment, dyke clast, and breccia matrix. (*c*) Flow foliation defined by alternating light and dark layers developed in the breccia matrix in an area of high clast concentration. Note the variable S0/S1 orientation within the argillite clasts. Mechanical pencil for scale. (*d*) Thin-section photomicrograph of the flow foliation, showing the compositionally different layers that define its structure. Note the quartz–feldspar aggregate in the bottom left hand corner and the fine-grained angular quartz clasts randomly distributed within the layers.

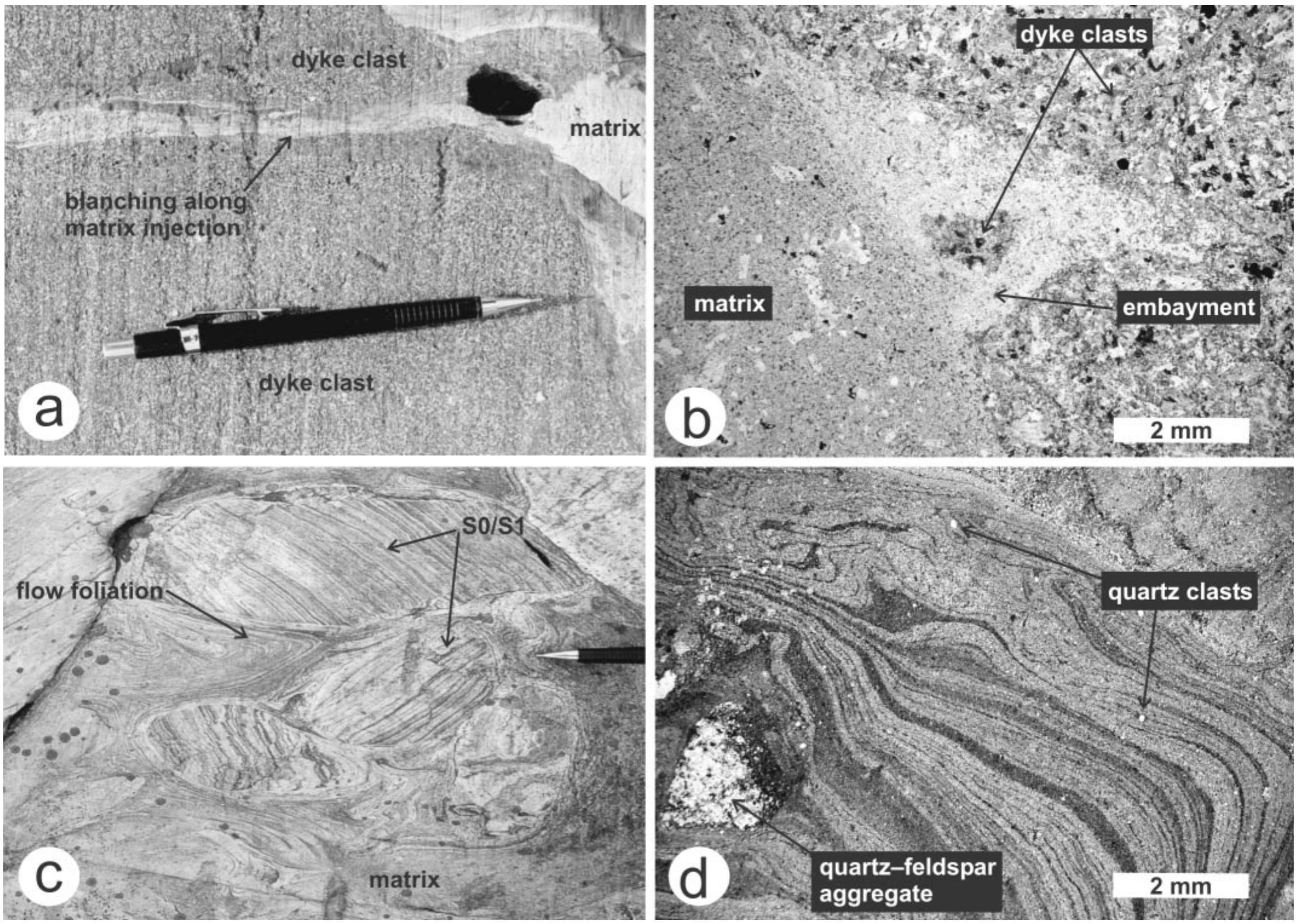

similar to that of the flow foliation. Very fine grained amphibolite clasts (<2 mm diameter) commonly exhibit biotite-poor, quartz-rich margins up to 20–30 µm wide, also with an average grain size of 2–5 µm (Fig. 7*f*).

Cataclastic zones

Prominent fracture zones are locally developed, commonly in proximity to a breccia pod (Fig. 5). They consist of pervasive, anastomosing fractures that offset bedding in the argillite but are overprinted by the S2 foliation (Fig. 8*a*). The fractures truncate both limbs of an S-shaped F2 fold and are themselves cut by breccia and overprinted by the axial-planar S2 foliation (Fig. 8*b*). Similar fracture patterns are also observed in argillite and amphibolite clasts within the breccia (Fig. 8*c*). S0/S1 within the argillite clasts is offset by the fractures, and both S0/S1 and the fractures are truncated sharply at the clast–matrix contact (Fig. 7*b*). There is no evidence of cataclastic fractures developed within the breccia matrix; rather, the breccia matrix intrudes fractures in the host argillite (Fig. 8*d*), in situ amphibolite dykes, and both argillite and amphibolite clasts (e.g., Fig. 6*a*). Small amounts of breccia matrix may develop along fracture planes where cataclasis is extreme.

Key timing relationships

The relative timing of brecciation can be determined from crosscutting and overprinting relationships.

(1) Host argillite (Fig. 4*a*) and argillite clasts (Fig. 7*b*) exhibit the S0/S1 composite foliation, whereas the breccia matrix does not. The random orientation of S0/S1 (Figs. 6*c*, 7*b*) in the clasts suggests some clast transport and rotation during the brecciation event. Brecciation, therefore, postdates both the development of S0/S1 and the D1 deformation event.

(2) Cataclastic fractures transect an F2 fold in the laminated argillite and are, in turn, truncated by the breccia matrix (Fig. 8*b*). Similar fractures within argillite clasts offset the S0/S1 composite foliation and are, themselves, truncated by the breccia matrix (Fig. 8*c*). These cataclastic fractures are absent in the breccia matrix. The fractured F2 fold, breccia

Fig. 7. Textural features and timing relationships within the host argillite and argillite and amphibolite clasts. (*a*) Rounded edge of the host argillite where breccia matrix branches around it. Note the S2 foliation (broken line) overprinting both the argillite and the breccia matrix, and the sharp contact between host and breccia matrix. Also note the distinctly dark breccia matrix supports several argillite clasts (C). (*b*) S0/S1 fabric in an argillite clast offset by brittle fractures (one example shown by broken line), which are themselves truncated at the breccia matrix contact. Note the blanched mantle surrounding the clast, the development of a flow-foliated matrix throughout, and the variable orientation of S0/S1 between the two clasts. Tip of mechanical pencil for scale. (*c*) F2 fold in an argillite clast (outlined by dotted line) that has been rotated during the brecciation event prior to S2 foliation (broken line) development. S2 transects both limbs of the fold. (*d*) Irregularly shaped amphibolite dyke clasts in the breccia matrix. Pencil for scale. (*e*) Contact between an amphibolite dyke clast and the breccia matrix. Note the lack of a chilled margin on the dyke clast (grain size consistently coarse from centre to margin). Tip of mechanical pencil for scale. (*f*) Thin-section photomicrograph of the corroded boundary around an amphibolite dyke clast showing the characteristic depletion of biotite and the development of a quartz-enriched halo.

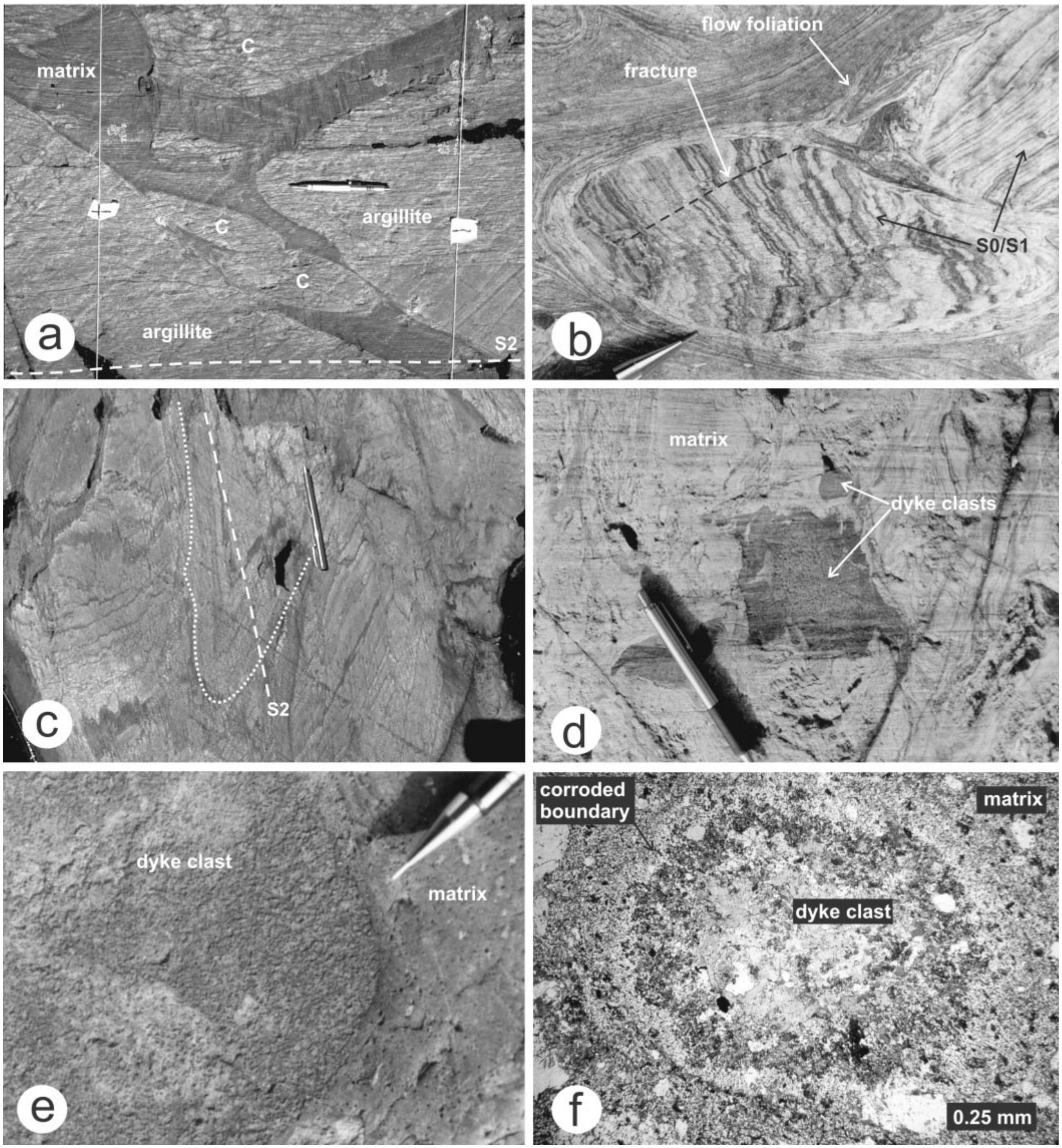

Fig. 8. Timing relationships and textural features of the breccias and cataclastic fracture zones. (*a*) Fractures, which offset a sandy layer in the laminated argillite, are overprinted by the S2 foliation (broken line). Tip of pen for scale. (*b*) The limb of an S-shaped F2 fold (defined by S0/S1 shown in heavy stipple) is truncated by a cataclastic fracture zone. The fractures are truncated at the breccia matrix contact, and the host argillite, the fractures, the breccia matrix, and the clasts are overprinted by the axial-planar S2 foliation. Pen for scale. (*c*) Cataclastic fractures developed in an argillite clast are truncated at the breccia matrix contact, while similar fractures are not developed in the breccia matrix. Pen for scale. (*d*) Breccia matrix developed, or injected, along cataclastic fracture planes in the host argillite (pen points to breccia matrix).

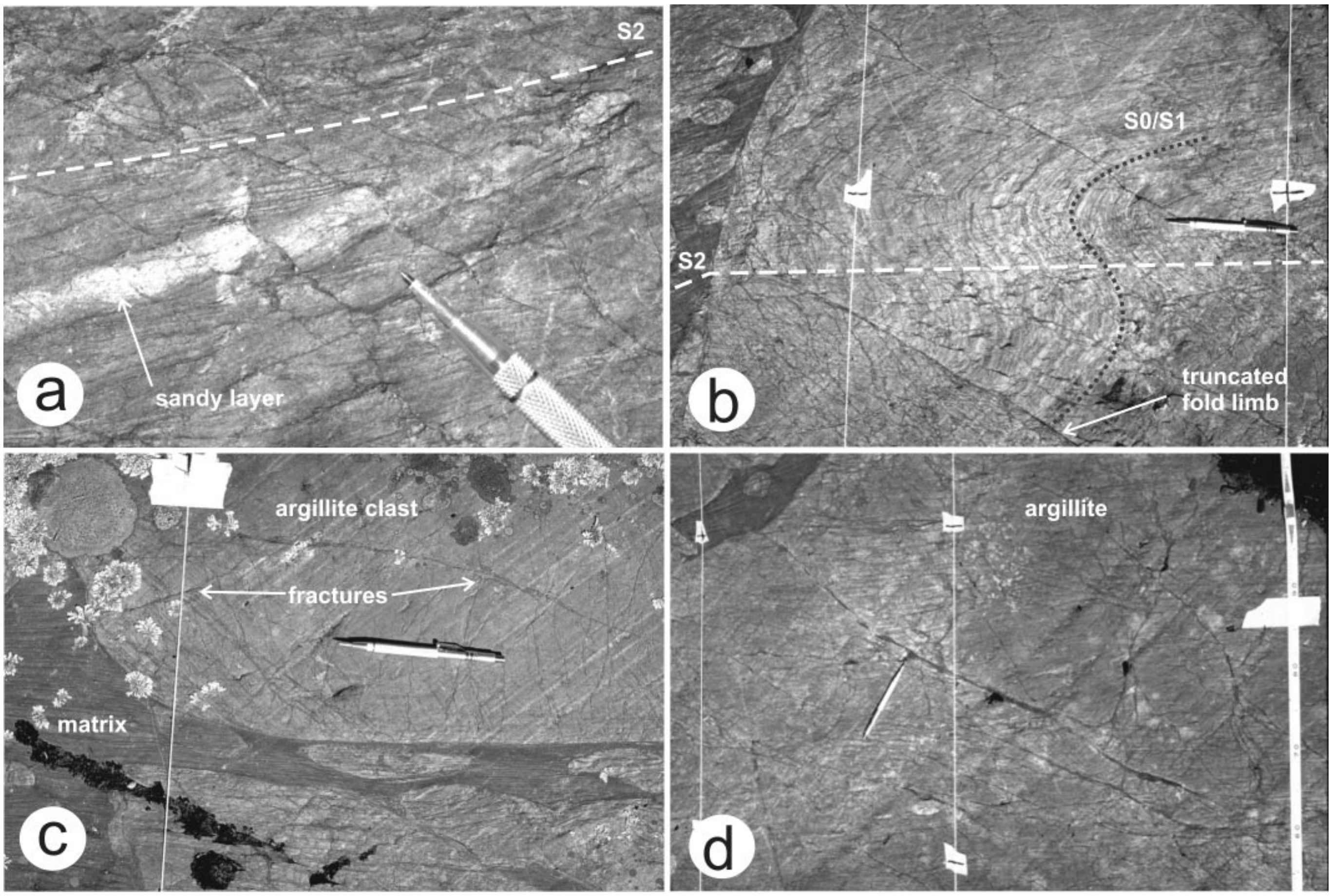

clasts, and unfractured breccia matrix are all overprinted by the S2 foliation (Fig. 8*b*). Brecciation, therefore, occurred during the D2 deformation event, after initial folding but before S2, the main regional fabric.

Discussion

The most common model for Sudbury breccia genesis associates breccia formation with the ca. 1850 Ma Sudbury impact event (Dressler 1984; Grieve et al. 1991; Thompson and Spray 1994). Similar breccias are found at other large impact sites such as the Vredefort structure in South Africa (Reimold and Colliston 1994) and the Ries structure in Germany (Pohl et al. 1977).

Alternatively, intrusion of Sudbury diabase dykes into consolidated rock may have induced brecciation at dyke – host rock contacts (Lowman 1999). This is based on contact and spatial relationships between certain Sudbury Breccia bodies and Sudbury diabase dykes, both north and south of the SIC, that are interpreted to reflect a temporal and genetic link. The breccias at Whitefish Falls could not have been formed in this manner, as the Sudbury dykes transect the central brecciated zone and the S2 foliation that overprints the breccias, and their north-northwest orientation exhibits no affinity to the distribution of breccia bodies (Fig. 3).

Shaw et al. (1999) attributed the Sudbury breccias in this area to the intrusion of pre-Nipissing diabase dykes into unconsolidated, wet Huronian sediment, suggesting that the amphibolite dykes (Fig. 3) are precursors to the regionally abundant Nipissing diabase intrusions. The amphibolite dykes, however, were previously associated with a suite of post-Nipissing diabase intrusions (Card 1984).

Shaw et al. (1999) interpreted soft-sediment deformation structures in the Gowganda Formation to be penecontemporaneous with amphibolite dyke intrusion and proposed a geochemical affinity between host rock, breccia, and dyke. Their hypothesis requires *all* pre- and syn-brecciation features to have formed within incompletely lithified sediment, prior to and during magma–sediment mixing.

Our study, however, documents the development of a penetrative composite foliation (S0/S1) and one generation of ductile folding (F2) in the host rock (argillite), prior to brecciation. Pre-brecciation brittle textures in the host argillite and the breccia clasts, such as offset S0/S1 compositional foliation and cataclastic fractures (Figs. 7*b*, 8*c*), also indicate that the host rock was competent prior to brecciation. The breccia matrix, completely lacking of similar fractures, must postdate the early ductile and brittle deformation. The lack of chilled margins on *all* amphibolite dyke clasts also argues against magma quenching in water-laden sediment.

The nature of the amphibolite dyke – host contact differs from intact to brecciated rock, within the same host (laminated argillite in Fig. 3). Dykes intruding intact argillite, on either side of the brecciated (high strain) zone (Fig. 3), exhibit sharp contacts with the host rock. Dykes within the breccia zone exhibit sharp to diffuse contacts often associated with the development of blanched clast margins (Fig. 6*a*) and irregular dyke clast shapes (Fig. 7*d*). The amphibolite dykes in the high-strain zone were, therefore, affected by deformation processes unlike those dykes outside of this zone. In addition, amphibolite clasts represent up to 3% of the lithic clasts in the breccia, but only where the breccias are spatially associated with amphibolite dykes in the adjacent host rock. The amphibolite dykes share no more of a causative relationship with brecciation than do the argillites. They were both simply in the destructive path of the brecciation mechanism.

A key observation with respect to potential brecciation models is the timing of breccia emplacement. We have demonstrated that the breccias formed after lithification and some deformation, and prior to overprint by a late tectonic fabric. We have ascribed pre-brecciation deformation to D1 and early D2, and post-brecciation deformation to late D2, D3, and D4. It is possible that the truncated F2 fold, overprinted by S2 (Fig. 8*b*), may represent two separate deformation events, with coincidental superposition of the later foliation exactly parallel to the axial plane of the earlier fold. There is no evidence, however, to support this interpretation. Our study indicates that D2 folding and fabric formation bracket the fracturing and brecciation event. Consequently, it is critical to determine the relationship between regional tectonism and D2.

D2: Penokean or not?

As noted earlier, the area was deformed during the Blezardian (ca. 2333–2219 Ma) and Penokean (ca. 1900–1700 Ma) orogenies (Fig. 2) (Bennett et al. 1991; Riller et al. 1999). Nipissing diabase sills transect both Blezardian-aged folds and late Blezardian soft-sediment deformation features (Card 1984; Bennett et al. 1991). Amphibolite dykes intrude the Nipissing diabase and transect major fold structures (Card 1984) and, therefore, also postdate the Blezardian orogeny. At Whitefish Falls, the same amphibolite dykes are folded and overprinted by a foliation related to local D2 deformation (Fig. 4*c*). Thus, D2 deformation must postdate the Blezardian orogeny. As there is no evidence of major Grenville-aged deformation in the Whitefish Falls area, all post-Blezardian deformation, including D2 and the brecciation event, must have occurred during the Penokean orogeny.

Zolnai et al. (1984) suggested that the development of a foliation, axial planar to Penokean-aged fold structures, is characteristic of late-stage Penokean deformation, which accounts for the protracted relationship between F2 folding, brecciation, and S2 foliation development.

Breccias at Whitefish Falls: a product of impact?

Regional occurrences of Sudbury breccia are the result of the Sudbury impact event (Dressler 1984; Thompson and Spray 1994), contemporaneous with Penokean deformation, and in agreement with our interpreted age of brecciation at Whitefish Falls (syn-D2). In the impact model for Sudbury breccias, breccia matrix and clasts are produced as a direct result of the combined processes of extreme cataclasis and friction melting in the mobilized rock (Spray and Thompson 1995). The resulting rock is often referred to as a pseudotachylyte, after Shand (1916) who described similar rocks around the Vredefort structure. Features and textures characteristic of pseudotachylyte development include embayed and partially digested host rock (Magloughlin 1992; Thompson and Spray 1996), a flow-foliated matrix (Thompson and Spray 1996), a highly rounded clast phase (Thompson and Spray 1996; Lin 1999), and an enrichment of ferromagnesian minerals in the matrix relative to the adjacent host rock (Maddock 1983; Spray 1992; Lin and Shimamoto 1998). Ferromagnesian minerals are preferentially mobilized, by comminution and melting, into the matrix because of their mechanical weakness, compared to more felsic components (e.g., quartz), thus creating a low-viscosity melt in which clasts and aggregates of quartz and feldspar are commonly preserved (Allen 1979; Maddock 1983; Magloughlin 1992). Whereas the brecciated host rock is depleted of ferromagnesian minerals, the overall ferromagnesian content of the brecciated and unbrecciated host rock, and breccia matrix, remains constant (Sibson 1975; Maddock 1983; Magloughlin 1992).

Host rock ferromagnesian mobilization and depletion, evident from embayed argillite–matrix contacts (Fig. 6*b*), may explain the relative abundance of quartz and feldspar clasts and aggregates compared with other mineral phases (Fig. 6*d*), and the high-degree of mineral segregation evident in flow-foliated breccia matrix (Figs. 6*c*, 6*d*, 7*b*). The blanched margins formed along matrix injections (Fig. 6*a*), along clast–matrix contacts (Figs. 6*c*, 7*b*), and around amphibolite dyke clasts (Fig. 7*f*) also appear to be a result of ferromagnesian mineral depletion. The high degree of roundness of lithic clasts (e.g., Figs. 6*c*, 7*f*) and similar rounding at argillite–matrix contacts (Fig. 7*a*) further suggest that melting occurred.

Combined development of each of these features strongly suggests that the breccias at Whitefish Falls are, therefore, pseudotachylytic in nature.

Melting and cataclasis of the different rock types within the breccia bodies would have served to chemically homogenize the breccia matrix. Therefore, the geochemical similarity between the in situ amphibolite dykes, amphibolite clasts, and breccia matrix, at Whitefish Falls (Shaw et al. 1999), is not unexpected.

Does the ring fit?

Superfaulting and regional brecciation

Superfaults at impact structures are characterized by large displacements during a single-slip event (Spray 1997). They are characterized by extremely high strain rates, a condition that occurs during the modification of the transient cavity in an impact event. These superfault structures are believed to host pseudotachylytic breccias that can define the multi-ring basin surrounding an impact site (Thompson and Spray 1994; Spray 1997). Landsat imagery was used to identify a distinct ring fracture 18–27 km from the SIC (Dressler et al. 1987) and to support the multi-ring basin model for Sudbury (Thompson and Spray 1994).

During superfaulting, fault surfaces act as activation planes that initiate frictional melting. Subsequently, this melt-laden material is injected into the host rock along preexisting weaknesses and fault-related fractures (Thompson and Spray 1996; Spray 1997). Based on the timing and textural relationships observed between the cataclastic fracture zones and the breccia bodies, we interpret brecciation at Whitefish Falls to have been initiated along a blind superfault caused by the Sudbury impact event. In the same time period, ductile deformation (D2) and reactivation of this fault served to focus strain along a narrow corridor (high-strain zone, Fig. 3), resulting in the attenuation and disruption of amphibolite dykes, transposition of the S0/S1 fabric, and development of an intense, penetrative S2 fabric. A preferential weakness in the host rock, corresponding to the high-strain zone (Fig. 3), did not predate brecciation.

Regional distribution of Sudbury breccia

Examples of Sudbury breccia, regionally distributed throughout the country rock, define the extent of the Sudbury Structure (Grieve et al. 1991). Examples of Sudbury Breccia have been found at 25, 40, and 80 km to the northwest in the Superior Province (Thompson and Spray 1994); in Huronian-aged sediments ~90 km to the northeast at Lake Temagami (Simony 1964); at the East Bull Lake and Shakespeare–Dunlop intrusions 25–40 km to the southwest (Chubb et al. 1994); and at Whitefish Falls, 70 km to the southwest (Fig. 1).

Throughout the Southern Province south of the SIC, any concentric ring structure is thought to have been obscured by post-impact tectono-metamorphism (Fig. 1) (Thompson and Spray 1996). Our study suggests that at Whitefish Falls, this is not the case. Here, the breccia zones cut discordantly across Penokean-aged (D2) fold structures and, therefore, postdate much of the regional shortening. Post-impact Penokean orogenesis produced the preferred alignment of breccia clasts and the S2 foliation overprint, but did not deform the Southern Province in the Whitefish Falls area sufficiently to obscure the breccia features. It is unlikely, therefore, that the proposed outer rings (Thompson and Spray 1994) were destroyed, and we suggest that moderately tectonized concentric rings are preserved south of the SIC, in the area of Whitefish Falls.

Our interpretation includes a southern extension of the proposed ring structure (Fig. 1) of Spray and Thompson (1995) to reflect the occurrence of impact-related breccia at Whitefish Falls. However, strike-slip movement along the Murray Fault Zone during post-brecciation Penokean shortening (Riller et al. 1999) has disrupted the continuity of this ring structure, and we have made no attempt to directly correlate the breccias at Whitefish Falls with those occurrences north of the fault (e.g., Thompson and Spray 1994).

Conclusions

Based on outcrop-scale and petrographic textural observations of breccia components, and the distribution of the breccia bodies with respect to neighbouring lithologies, our study suggests that the breccias at Whitefish Falls share no genetic link with either the Nipissing diabase or Sudbury diabase dykes. We suggest that brecciation at Whitefish Falls is penecontemporaneous with the Penokean orogeny, and likely a result of the Sudbury impact event. Crosscutting relationships indicate a close temporal association between cataclastic fracture development and brecciation. We propose that these enigmatic breccias resulted from the Sudbury impact event by injection of a pseudotachylytic melt that was generated and mobilized along a blind superfault in the Whitefish Falls area. Reactivation of this superfault, during continued Penokean deformation, produced the high-strain zone that overprints and spatially coincides with the breccias.

Acknowledgments

This paper is an expansion of Parmenter's B.Sc. Honours thesis, which was supervised by Lee and Coniglio and completed during Parmenter's M.Sc. thesis work as a student of S. Lin. The research was supported by Natural Sciences and Engineering Research Council of Canada grants to Coniglio and Lin. S. Lin provided constructive comments on an earlier version of this manuscript. This manuscript benefitted greatly from formal reviews by R.A.F. Grieve and J.G. Spray.

References

Allen, A.R. 1979. Mechanism of frictional fusion in fault zones. Journal of Structural Geology, **1**: 231–243.

Bennett, G., Dressler, B.O., and Robertson, J.A. 1991. The Huronian Supergroup and associated intrusive rocks. *In* Geology of Ontario. *Edited by* P.C. Thurston, H.R. Williams, R.H. Sutcliffe, and G.M. Stott. Geological Survey of Canada, Special Volume 4, pp. 549–592.

Card, K.D. 1978. Geology of the Sudbury–Manitoulin area, districts of Sudbury and Manitoulin. Ontario Geological Survey, Report 166.

Card, K.D. 1984. Geology of the Espanola – Whitefish Falls area, District of Sudbury, Ontario. Ontario Geological Survey, Report 131.

Chubb, P.T., Vogel, D.C., Peck, D.C., James, R.S., and Keays, R.R. 1994. Occurrences of pseudotachylyte at the East Bull Lake and Shakespeare–Dunlop intrusions, Ontario, Canada. Canadian Journal of Earth Sciences, **31**: 1744–1748.

Condie, K.C., Bobrow, D.J., and Card, K.D. 1987. Geochemistry of Precambrian mafic dykes from the southern Superior Province of the Canadian Shield. *In* Mafic dyke swarms. *Edited by* H.C. Halls and W.F. Fahrig. Geological Association of Canada, Special Paper 34, pp. 95–108.

Corfu, F., and Andrews, A.J. 1986. A U–Pb age for mineralized Nipissing Diabase, Gowganda, Ontario. Canadian Journal of Earth Sciences, **23**: 107–109.

Dietz, R.S. 1964. Sudbury Structure as an astrobleme. Journal of Geology, **72**: 412–434.

Dressler, B.O. 1979. Geology of the Emo, Rhodes, and Botha Townships, District of Sudbury. Ontario Geological Survey, Report 196, pp. 54.

Dressler, B.O. 1984. The effects of the Sudbury event and the intrusion of the Sudbury Igneous Complex on the footwall rocks of the Sudbury Structure. *In* The geology and ore deposits of the Sudbury Structure. *Edited by* E.G. Pye, A.J. Naldrett, and P.E. Giblin. Ontario Geological Survey, Special Volume 1, pp. 97–136.

Dressler, B.O., Morrison, G.G., Peredery, W.V., and Rao, B.V. 1987. The Sudbury Structure, Ontario, Canada — a review. *In* Research in terrestrial impact structures. *Edited by* J. Pohl. Friedr. Vieweg & Sohn, Braunschweig–Weisbaden, pp. 39–68.

Frarey, M.J., Loveridge, W.D., and Sullivan, R.W. 1982. A U–Pb zircon age for the Creighton granite, Ontario. *In* Rb–Sr and U–Pb isotopic age studies, Report 5. Geological Survey of Canada, Paper 81-1C, pp. 129–132.

Grieve, R.A.F., Stoeffler, D., and Deutsch, A. 1991. The Sudbury Structure: controversial or misunderstood? Journal of Geophysical Research, **96**: 22 753 – 22 764.

Krogh, T.E., Davis, D.W., and Corfu, F. 1984. Precise U–Pb zircon and baddeleyite ages for the Sudbury area. *In* The geology and ore deposits of the Sudbury Structure. *Edited by* E.G. Pye, A.J. Naldrett, and P.E. Giblin. Ontario Geological Survey, Special Volume 1, pp. 431–448.

Krogh, T.E., Corfu, F., Davis, D.W., Dunning, G.R., Heaman, L.M., Kamo, S.L., Machado, N., Greenough, J.D., and Nakamura, E. 1987. Precise U–Pb isotopic ages of diabase dykes and mafic to ultramafic rocks using trace amounts of baddeleyite and zircon. *In* Mafic dyke swarms. *Edited by* H.C. Halls and W.F. Fahrig. Geological Association of Canada, Special Paper 34, pp. 147–152.

Krogh, T.E., Kamo, S.L., and Bohor, B.F. 1996. Shocked metamorphosed zircons with correlated U–Pb discordance and melt rocks with concordant protolith ages indicate an impact origin for the Sudbury Structure. *In* Earth processes: reading the isotopic code. American Geophysical Union, Monograph 95, pp. 343–352.

Lin, A. 1999. Roundness of clasts in pseudotachylytes and cataclastic rocks as an indicator of frictional melting. Journal of Structural Geology, **21**: 473–478.

Lin, A., and Shimamoto, T. 1998. Selective melting processes as inferred from experimentally generated pseudotachylytes. Journal of Asian Earth Sciences, **16**: 533–545.

Lowman, P.D., Jr. 1999. Original size of the Sudbury Structure: evidence from field investigations and imaging radar. Geological Association of Canada – Mineralogical Association of Canada, Program with Abstracts, **24**: 74.

Maddock, R.H. 1983. Melt origin of fault-generated pseudotachylytes demonstrated by textures. Geology, **11**: 105–108.

Magloughlin, J.F. 1992. Microstructural and chemical changes associated with cataclasis and frictional melting at shallow crustal levels: the cataclasite–pseudotachylyte connection. Tectonophysics, **204**: 243–260.

Peredery, W.V., and Morrison, G.G. 1984. Discussion of the origin of the Sudbury Structure. *In* The geology and ore deposits of the Sudbury Structure. *Edited by* E.G. Pye, A.J. Naldrett, and P.E. Giblin. Ontario Geological Survey, Special Vol. 1, pp. 491–511.

Pohl, J., Stoeffler, D., Gall, H., and Ernstson, K. 1977. The Ries impact crater. *In* Impact and explosion cratering: planetary and terrestrial implications. *Edited by* D.J. Roddy, R.O. Pepin, and R.B. Merrill. Pergamon Press, New York, pp. 343–404.

Reimold, W.U., and Colliston, W.P. 1994. The pseudotachylites of the Vredefort Dome and the surrounding Witwatersrand Basin, South Africa. *In* Large meteorite impacts and planetary evolution. *Edited by* B.O. Dressler, R.A.F. Grieve, and V.L. Sharpton. Geological Society of America, Special Publication 293, pp. 177–196.

Riller, U., Schwerdtner, W.M., Halls, H.C., and Card, K.D. 1999. Transpressive tectonism in the eastern Penokean orogen, Canada: consequences for Proterozoic crustal kinematics and continental fragmentation. Precambrian Research, **93**: 51–70.

Rousell, D.H., Gibson, H.L., and Jonasson, I.R. 1997. The tectonic, magmatic, and mineralization history of the Sudbury Structure. Exploration and Mining Geology, **6**: 1–22.

Shand, S.J. 1916. The pseudotachylyte of Parijs (Orange Free State) and its relation to “trap-shotten gneiss” and “flinty crush rock.” Quarterly Journal of the Geological Society of London, **72**: 198–221.

Shaw, C.S.J., Young, G.M., and Fedo, C.M. 1999. Sudbury-type breccias in the Huronian Gowganda Formation near Whitefish Falls, Ontario: products of diabase intrusion into incompletely consolidated sediments? Canadian Journal of Earth Sciences, **36**: 1435–1448.

Sibson, R. 1975. Generation of pseudotachylyte by ancient seismic faulting. Geophysical Journal of the Royal Astronomical Society, **43**: 775–794.

Simony, P.S. 1964. Geology of the northwestern Lake Temagami area, District of Nipissing. Ontario Department of Mines, Geological Report 28.

Spray, J.G. 1992. A physical basis for the frictional melting of some rock-forming minerals. Tectonophysics, **205**: 19–34.

Spray, J.G. 1997. Superfaults. Geology, **25**: 579–582.

Spray, J.G., and Thompson, L.M. 1995. Friction melt distribution in a multi-ring impact basin. Nature (London), **373**: 130–132.

Stockwell, C.H. 1982. Proposals for the time classification and correlation of Precambrian rocks and events in Canada and adjacent areas of the Canadian Shield. Geological Survey Canada, Paper 80-19.

Thompson, L.M., and Spray, J.G. 1994. Pseudotachylytic rock distribution and genesis within the Sudbury impact structure. *In* Large meteorite impacts and planetary evolution. *Edited by* B.O. Dressler, R.A.F. Grieve, and V.L. Sharpton. Geological Society of America, Special Publication 293, pp. 275–287.

Thompson, L.M., and Spray, J.G. 1996. Pseudotachylyte petrogenesis: constraints from the Sudbury impact structure. Contributions to Mineralogy and Petrology, **125**: 359–374.

Young, G.M. 1983. Tectono-sedimentary setting of the early Proterozoic rocks of the northern Great Lakes region. *In* Early Proterozoic geology of the Great Lakes region. *Edited by* G. Medaris Jr. Geological Society of America, Memoir 160, pp. 15–32.

Zolnai, A.I., Price, R.A., and Helmsteadt, H. 1984. Regional cross section of the Southern Province adjacent to Lake Huron, Ontario: implications for the tectonic significance of the Murray Fault Zone. Canadian Journal of Earth Sciences, **21**: 447–456.